

Article

Not peer-reviewed version

Anion Complexation by an Azocalix [4]Arene Derivative and the Scope of Its Fluoride Complex Salt to Capture CO₂ from the Air

[ANGELA FATIMA DANIL DE NAMOR](#)^{*} and Nawal Al Hakawati

Posted Date: 14 July 2023

doi: 10.20944/preprints202307.0987.v1

Keywords: Azocalix[4]arene; Fluoride complex salt; Carbon dioxide capture



Preprints.org is a free multidiscipline platform providing preprint service that is dedicated to making early versions of research outputs permanently available and citable. Preprints posted at Preprints.org appear in Web of Science, Crossref, Google Scholar, Scilit, Europe PMC.

Copyright: This is an open access article distributed under the Creative Commons Attribution License which permits unrestricted use, distribution, and reproduction in any medium, provided the original work is properly cited.

Article

Anion Complexation by an Azocalix [4]Arene Derivative and the Scope of Its Fluoride Com-Plex Salt to Capture CO₂ from the Air

Angela F Danil de Namor ^{1,*} and Nawal Al Hakawati ²

¹ Laboratory of Thermochemistry, School of Chemistry and Chemical Engineering, University of Surrey, Guildford, Surrey GU2 7XH

² Department of Biological Sciences, Faculty of Science, Beirut Arab University, Tripoli, Lebanon; n.elhakawati@bau.edu.lb

* Correspondence: a.danil-de-namor@surrey.ac.uk; Tel.: +44 1483 689581

Abstract: A newly synthesized upper rim azocalix[4]arene, namely, 5,11,17,23-tetra[(4-ethylacetoxypheyl)(azo)]calix[4]arene, CA-AZ was fully characterized and its chromogenic and selective properties for anions are reported. The receptor is selective for the fluoride anion and its mode of interaction in solution is discussed. The kinetics of the complexation process was found to be very fast as reflected in the immediate color change observed with a naked eye resulting from the receptor-anion interaction. Emphasis is made about the relevance in selecting a solvent in which the formulation of the process is representative of the events taking place in the solution. The composition of the fluoride complex investigated by UV/VIS spectrophotometry, conductance measurements and titration calorimetry was 1:1 and the thermodynamics of complexation was determined. The fluoride complex salt was isolated, and a detailed investigation was carried out to assess its ability to remove CO₂ from the air. Recycling of the complex was easily achieved. Final conclusions are given.

Keywords: azocalix[4]arene; fluoride complex salt; carbon dioxide capture

1. Introduction

Carbon dioxide among all gases has been an issue of extensive political debate due to its importance as a greenhouse gas [1–3] which is a key cause of global warming. In addition to its environmental impact, the gas has been employed in the chemical industry, food, modern agriculture, and medical diagnosis due to its vital role in human physiology. Hence, the development of new methodology for the selective, quantitative, and rapid recognition of this inert gas [4–7] is a matter of priority concern. Methods such as gas chromatography, infrared spectroscopy, and electrochemistry (Severing Haus electrodes) are used to detect CO₂. More recently, few attempts have been made to develop optical chemo sensors based on UV spectroscopy, colorimetry, or fluorescence to sense carbon dioxide [8–11]. Interestingly, few studies have shown that chemo sensor compounds displaying high selectivity for the fluoride anion were able to detect carbon dioxide gas with full restoration of their original colors and spectral properties [12,13]. Xia and co-workers reported the carboxylation of pyrimido[1,2] benzimidazole and squarine derivatives by the aid of carbon dioxide in the presence of an excess of a fluoride salt [Bu₄N] F [14,15].

Encouraged by the single step procedure introduced by Gutsche [16] for the synthesis of parent calix[n]arenes, for several years we have been focused on thermodynamic aspects of calixarene chemistry [17], mainly narrow rim functionalized calixarenes [18–21]. Recently we have proceeded with an investigation on wide rim calixarene derivatives involving azo functionalities. The design of chromoionophores with multifunctional sensor systems attracted much attention due to their usefulness in the development of chemical sensors [22]. These sensors exhibit color changes as they interact with ionic or molecular species [23,24] which can be easily detected with the naked eye without the use of any spectroscopic technique. More particularly, azophenol based chemo sensors have been widely incorporated into the chromoionophores. These compounds can display a change

in their absorption spectra in addition to a color change upon interaction with metal cations [25–30] or anions [31–42]. A series of non-macrocyclic azophenol derivatives as chromogenic units designed to selectively generate color change as they complex with different anions have been reported by Hong and co-workers [31–34].

The introduction of the azo functionality in macrocyclic compounds has been reviewed by Wagner-Wysiecka and co-workers in 2018 [43]. Much attention has been devoted to the development of fast sensors for analyzing fluoride due to the anion dual functionality whether in the treatment of osteoporosis and prevention of dental decay, fluorosis, or other bone diseases like osteosarcoma [44–47].

Most of the work carried out in the field of Supramolecular Chemistry has been mainly concerned with complexation studies involving ionic and neutral species with little attention on the properties of these new complex salts and their applications. CO₂ fixation has been elegantly investigated in solution and in the solid state by Bazzicalupi and coworkers [48] using copper (II) and zinc (II) complexes of [15]aneN₃O₂ macrocycles, however there are no reports on CO₂ uptake by anion complex salts of calix[4]arene in solution and in the air. Hence we report here an easily recyclable chemo sensor probe for the detection and capture of CO₂ in air based on the tetra-*n*-butyl ammonium *para*-ester diazo phenyl calix[4]arene fluoride salt, Bu₄N [CA-AZ F]. In doing so fundamental studies on the synthesis and characterization of the free receptor, *para*-ester diazo phenyl calix[4]arene, CA-AZ and its complexing properties in solution are also included.

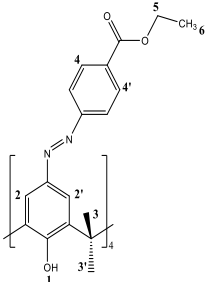
2. Results and Discussion

2.1. Structural characterization of 5,11,17,23-tetra[(4-ethylacetoxypheyl) (azo)]calix[4]arene (CA-AZ)

2.1.1. ¹H NMR characterization of CA-AZ in DMSO-d₆ and CDCl₃ at 298 K.

¹H NMR analyses of CA-AZ in DMSO-d₆ and CDCl₃ were done to identify its conformational morphism and the changes that it undergoes upon interaction with guest species. Gutsche [16] has stated that the difference in the chemical shifts ($\Delta\delta_{\text{ax-eq}}$, ppm) between the low and high field pairs of resonances arising from the methylene protons (H-equatorial H-3 and axial H-3') of the calix[4] based receptor provides a measure of the 'flattening' of the 'cone'. Thus, for a ligand in a perfect 'cone' conformation the $\Delta\delta_{\text{ax-eq}}$, 0.90 ppm, and decreases significantly in the 'flattened' conformation or increases when the aromatic rings become more parallel to each other and the macrocyclic adopts a distorted 'cone' conformation. Considering the above statements, the almost 'cone' conformational morphism of CA-AZ was detected in DMSO-d₆ where the $\Delta\delta_{\text{ax-eq}}$ = 0.83 ppm. In CDCl₃, a flattened 'cone' conformation with $\Delta\delta$ = 0.53 ppm is found. Also, it should be mentioned that the ligand exhibited a red color in DMSO-d₆.

Table 1. ¹H NMR data for CA-AZ in deuterated solvents at 298 K (CDCl₃ was selected as a reference solvent).



| δ (ppm) | | | | | | | | |
|---------------------|-------|--------|---------------------|-----------------|-------|-------|-------|-------|
| Solvent | H-1 | H-2,2' | H-3 H-equatorial | H-3' H-axial | H-4 | H-4' | H-5 | H-6 |
| CDCl ₃ | 10.25 | 7.85 | 3.87 | 4.40 | 8.13 | 8.14 | 4.39 | 1.4 |
| DMSO-d ₆ | - | 7.82 | 3.51 | 4.34 | 7.85 | 8.05 | 4.31 | 1.32 |
| $\Delta\delta$ | - | -0.03 | -0.36 | -0.06 | -0.28 | -0.09 | -0.08 | -0.08 |

[CA-AZ] = 2.17×10^{-4} mol.dm⁻³; V = 0.5cm³.

2.1.2. FT-ATR characterisation of para-ester diazophenylcalix[4]arene

The infrared spectrum of CA-AZ is shown in Figure 1. The broad band at 3221 cm^{-1} is assigned to the -OH stretching vibrations of the phenol ring which is within the $3100\text{--}3500\text{ cm}^{-1}$ range found for all parent calixarenes [49]. The lower position of the OH stretch vibration may be attributed to hydrogen bond formation in the narrow rim as previously found for these macrocycles [49]. The strong band at 1713 cm^{-1} in the spectrum of CA-AZ corresponds to the C=O stretching vibration [50]. The N=N stretching mode appears in the region of 1467 cm^{-1} [50]. The weak band at 1362 cm^{-1} is attributed to the aryl group [50]. The C-O stretching mode is represented by an intense band at 1266 cm^{-1} .

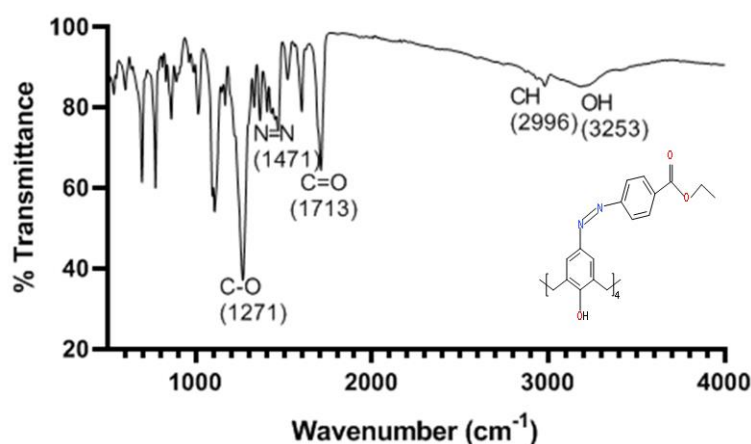


Figure 1. Infrared spectrum of CA-AZ displaying the most important bands of the ligand.

2.1.3. Thermal stability of para-ester diazophenylcalix[4]arene

An important parameter that should be determined is the thermal stability of the ligand as it is relevant for its applications. This was investigated through thermogravimetric analysis where the TG curve is presented in Figure 2. The curve below shows that the ligand can preserve thermal stability up to 280°C . Two exothermic phases are shown in *para*-ester diazophenylcalix[4]arene TG curve. The first one corresponds to the release of moisture from the surface (average experimental mass loss of 15.39 %) followed by the second one indicating the decomposition of the whole compound with an average mass loss of 57.12 %.

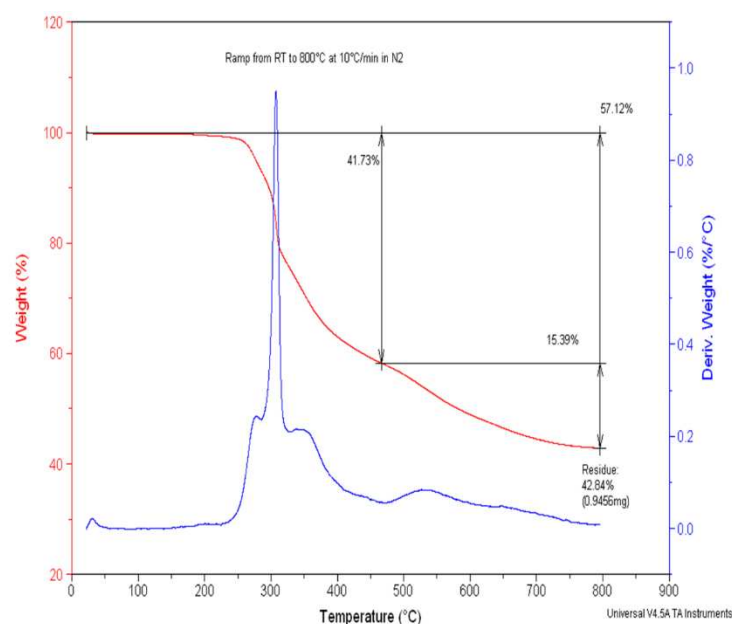


Figure 2. The TG curve of CA-AZ.

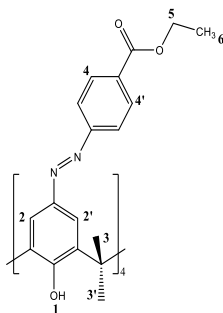
2.2. ¹H NMR complexation of CA-AZ with anions in DMSO-d₆ at 298 K.

DMSO was the selected solvent for further experimental work, given that in chloroform, anion salts are predominantly as ion pairs.

Screening experiments were conducted to determine the selectivity of CA-AZ to different ionic species (cations and anions). Based on the ¹H NMR findings, the ligand showed no interactions with alkali, alkaline-earth, and transition metal ions where no chemical shift changes were observed. Chemical shift values (δ in ppm) of CA-AZ with F⁻, H₂PO₄⁻, HSO₄⁻ and Cl⁻ as tetra-n-butyl ammonium salts and CO₃²⁻ as ammonium salt are all listed along with the free ligand in Table 2. Besides, color changes from faint red to dark purple and dark red were observed immediately after the addition of F⁻ and H₂PO₄⁻ salts (1 × 10⁻³ mol dm⁻³) respectively to CA-AZ.

As shown in Table 2, some protons (H-2, H-4, H-4' and H-5) showed severe broadness to the extent that they did not show up in the spectrum upon the addition of F⁻. Quite clearly from the Δδ_{ax-eq} values of the free and complex CA-AZ, the addition of the F⁻ salt produces a dramatic conformational change in which the ligand adopts a 'flattened' cone conformation suggesting that the intramolecular hydrogen bonding between the hydroxyl group(-OH) in the narrow rim of the free receptor is broken as a result of the receptor-anion interaction.

Table 2. ¹H NMR chemical shift changes (Δδ, ppm) resulting from addition of anion salts (as tetra-n-butyl ammonium) to CA-AZ relative to the free ligand in DMSO-d₆ at 298 K.



| δ (ppm) | | | | | | | |
|---|-----|-------|-------|-------|-------|-------|-------|
| | H-1 | H-2 | H-3 | H-3' | H-4 | H-4' | H-5 |
| δ _{Ref} | - | 7.82 | 3.51 | 4.34 | 7.85 | 8.05 | 4.3 |
| F ⁻ | - | - | -0.19 | -0.64 | - | - | - |
| CO ₃ ²⁻ | - | -0.2 | 0.12 | 0.28 | -0.1 | -0.08 | 0.0 |
| H ₂ PO ₄ ⁻ | - | -0.17 | - | 0.3 | -0.09 | -0.06 | 0.0 |
| HSO ₄ ⁻ | - | -0.01 | -0.18 | 0.6 | 0.0 | 0.0 | 0.0 |
| Cl ⁻ | - | 0.02 | 0.17 | 0.08 | 0.0 | 0.0 | -0.08 |

[X⁻] = 1.10 × 10⁻³ mol.dm⁻³; V = 0.5 cm³; [CA-AZ] = 2.17 × 10⁻⁴ mol.dm⁻³; V = 0.5 cm³.

The conformational changes that CA-AZ undergoes with H₂PO₄⁻ could not be calculated due to the broadening of the equatorial (H-3) signal. As far as HSO₄⁻ is concerned the change is significant with the macrocycle adopting a 'distorted' 'cone' as reflected in the Δδ_{ax-eq} value of 1.57 ppm. This is in contrast with the Δδ_{ax-eq} of 0.70 ppm found for the CA-AZ-Cl⁻ where the macrocycle adopts a slightly 'flattened' conformation much less pronounced than that observed for the fluoride complex. Deshielding of the equatorial and axial protons (H-3 and H-3') changed the Δδ_{ax-eq} value from 0.83 ppm to 0.99 ppm as a result of the CA-AZ- CO₃²⁻ interaction.

Up-field shifts in the aromatic protons (H-2 and H-4) of CA-AZ were observed upon complexation with H₂PO₄⁻, while those for CA-AZ-HSO₄⁻ and CA-AZ-Cl⁻ complexes remain unchanged. Up-field shifts in H-6 (methylene proton) of the same magnitude were detected for the three complexes except for CO₃²⁻ (ammonium counter-ion). Three signals for tetra-n-butyl ammonium counter ion were shown. Interestingly, the intensities of tetra-n-butyl ammonium peaks in the spectrum of CA-AZ-F⁻ complex are lower than those involving other anions. The same finding

of H-6 chemical shift was obtained but with different counter ion. ^1H NMR complexation analysis of CA-AZ with NaF in DMSO- d_6 was unclear due to the very low solubility of the salt in DMSO- d_6 . Up-field shift of the aromatic protons (H-2 and H-4) was observed in the ^1H NMR spectrum of CA-AZ- CO_3^{2-} complex. Moreover, these peaks became broad as soon as an interaction between CA-AZ and CO_3^{2-} through hydrogen-bonding formation takes place. It is expected that the aromatic peaks will continue to broaden with further addition of CO_3^{2-} until they disappear. The interaction of CO_3^{2-} with CA-AZ yielded a slight change in the ligand conformation. No changes in the chemical shifts of the ligand were observed from ^1H NMR studies of CA-AZ and NaNO_3 in DMSO- d_6 .

^1H NMR studies suggest that the ligand selectivity for anions follows the sequence, $\text{F}^- > \text{H}_2\text{PO}_4^- > \text{CO}_3^{2-} > \text{HSO}_4^- > \text{Cl}^-$ while the sensitivity of CA-AZ to F^- , H_2PO_4^- and CO_3^{2-} respectively is evident from the color changes that the receptor underwent in the presence of these anions.

2.3. Chromogenic properties and UV-VIS experiments

CA-AZ possesses dual functionality for its selectivity for a given ion through the phenolic hydroxyl binding sites and its sensitivity as a chemo sensor with covalently linked azo moieties.

The sensitivity function was determined from the chromogenic properties of the ligand upon its complexation with different ionic species in DMSO (Figure 3) along with the spectral changes in the UV-VIS analysis (Figure 4). Colour changes from yellow to purple and red were detected immediately after the addition of F^- and H_2PO_4^- (1×10^{-4} mol. dm^{-3} as tetra-*n*-butyl ammonium salt) to CA-AZ (1×10^{-5} mol. dm^{-3}) in DMSO. However, the addition of higher concentrations of these anion salts turned the colour even darker (dark blue in the case of F^- and maroon, red with H_2PO_4^-). Moreover, a change in the colour from yellow to orange was observed with CO_3^{2-} (ammonium counter-ion). No visible changes in the colour of CA-AZ were detected with addition of HSO_4^- and Cl^- (Figure 4).



Figure 3. Colour changes of CA-AZ resulting from anion interactions in DMSO.

Several studies reported two possible tautomeric forms of azocalix[4]arenes [51–54], azophenol and quinone-hydrazone through which they possess different visible spectral features and this is also dependant on the substituents of the azocalix[4]arene derivatives [55]. In the case of CA-AZ, the absorption maxima (λ_{max}) in the UV-spectrum are observed at 384 nm which corresponds to a π - π^* transition suggesting that the ligand exists in the azophenol form [56]. However, visible spectral changes of CA-AZ were observed with the addition of F^- and H_2PO_4^- from 384 nm to 501 nm with shoulders at 561 and 393 nm respectively. A marked bathochromic shift is found for F^- with an isosbestic point at 433 nm. This spectral change corresponds to a n - π^* transition indicating the presence of CA-AZ in a quinone-hydrazone tautomeric form. Chawla and Gupta [57] suggested a charge transfer induced to the acidic ligand protons *via* the addition of basic F^- salt. Moreover, azophenol chromophore electron excitation occurs through charge transfer from the phenol (oxygen donor atoms) to the substituents of the chromophore unit (acceptor atoms) which results in a colour change [58]. Chen and co-workers [59] reported similar findings with calix[4]arene derivatives for anion chromogenic sensors. Thiampanya and co-workers [60] reported a charge transfer in an azocalix[4]arene strapped calix[4]pyrrole from the donor oxygen atom of the azophenol moiety to the acceptor atom in the chromophore substituent following addition of basic anions. The outcome of this investigation indicates that CA-AZ is more sensitive to F^- than the remaining anions where a significant visible spectral shift was observed by addition of this anion to the ligand.

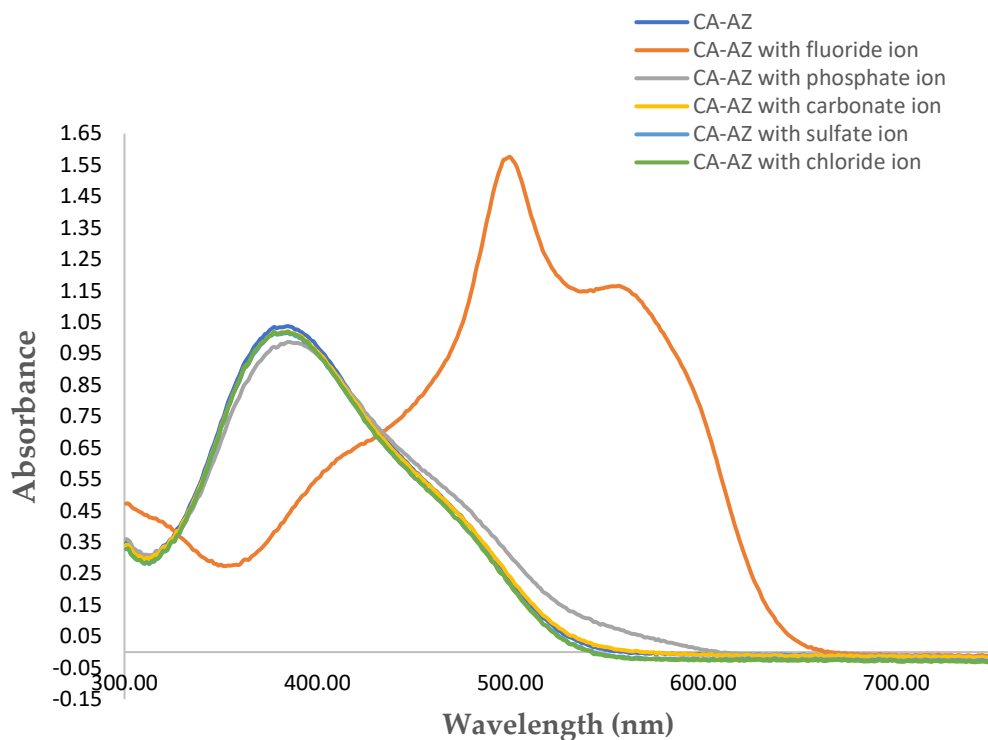


Figure 4. Spectral changes of *para*-ester diazophenylcalix[4]arene (1×10^{-5} mol.dm⁻³) with different anions.

Given that the aim of this paper is to isolate the fluoride complex salt we proceeded with ¹H NMR titration of CA-AZ with the fluoride anion salt in DMSO-d₆ as well as UV-Visible spectroscopy, conductance measurements and titration calorimetry to determine the composition of the fluoride complex salt and its stability.

2.4. ¹H NMR titration of *para*-ester diazophenylcalix[4]arene with fluoride anion as tetra-*n*-butyl ammonium in DMSO-d₆

Knowing that CA-AZ exhibits sensitivity and selectivity for F⁻, ¹H NMR titration of the ligand with the fluoride anion salt in DMSO-d₆ was carried out to gain more insights on its binding mode. ¹H NMR spectra in Figure 5 reveals the mode of interaction of CA-AZ with the anion. As the addition of TBAF (tetra-*n*-butyl ammonium fluoride) progresses, the peaks corresponding to the aromatic protons (**H-2**, **H-4** & **H-4'**) and ethyl proton (**H-5**) along with the equatorial and axial protons became more broaden until they almost disappeared but not shifted at all. From the ¹H NMR titration outcomes, it becomes clear that further addition of fluoride to CA-AZ leads to a deprotonation of one of the phenolic OH functionality in the narrow rim of the receptor. This statement is in agreement with the findings by Zheng and co-workers [61]. These authors demonstrated that upon addition of higher concentrations of F⁻ in the ¹H NMR titration of a calix[4]arene derivative resulted in the disappearance and very small chemical shifts in the characteristic peaks of the receptor.

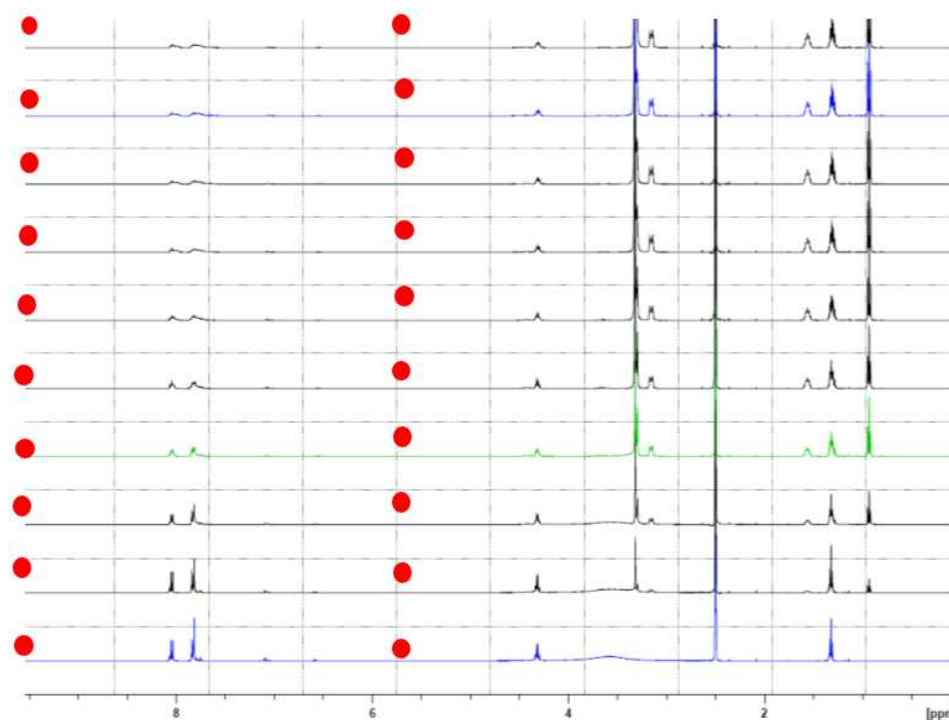


Figure 5. ^1H NMR spectral changes of CA-AZ titrated with 0.36 equivalents of F^- at 298 K.

This mode of interaction between the ligand and F^- is highly dependent on the concentration of both, in the medium. However, when the concentration of the ligand or the F^- varies, different interaction behaviour will be observed as in the case of ^1H NMR complexation of CA-AZ and F^- where the fluoride salt was in excess of the receptor (Table 2).

2.5. UV-VIS titration of CA-AZ with the fluoride anion salt in DMSO

Figure 6 shows that as the concentration of fluoride increases the absorbance increases until the [CA-AZ: F^-] ratio is 1:1. Then the absorbance remains constant. However, the addition of F^- turned the colour from yellow to faint pink which was not altered by further addition of the fluoride salt.

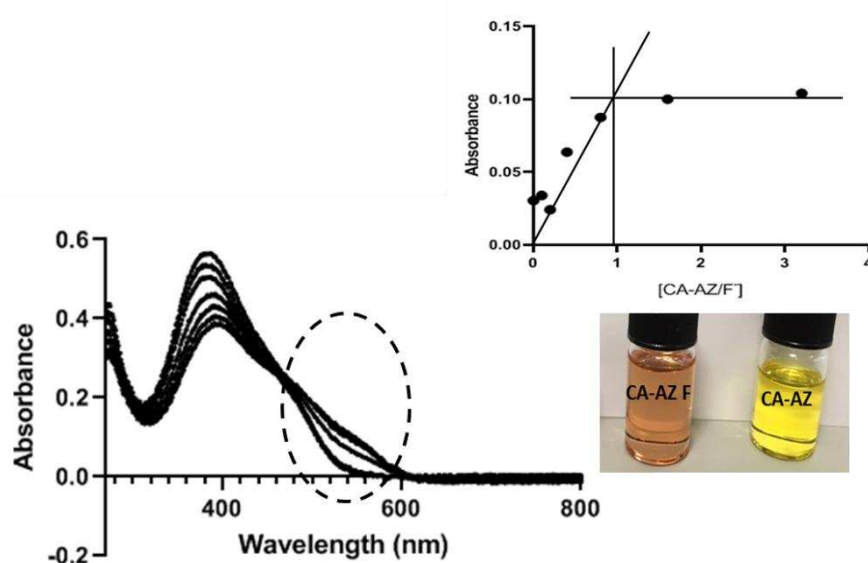


Figure 6. Plot of absorbance at 530 nm as a function of $[\text{CA-AZ}]/[\text{F}^-]$ resulting from the UV-VIS titration of CA-AZ with F^- in DMSO.

2.6. Conductometric studies of CA-AZ interacting with fluoride anion in DMSO at 298.15 K

Conductometric titration experiments were carried out to have further evidence of the composition of the complex (Figure 7). There is a slight change in conductance from A to B due to the complexation with a significant increase from B to C due to the excess of fluoride ions in solution. A well-defined change in the curvature is observed at the reaction stoichiometry suggesting the formation of a 1:1 complex. This outcome of conductance measurements agrees with that obtained by the UV-VIS spectroscopy.

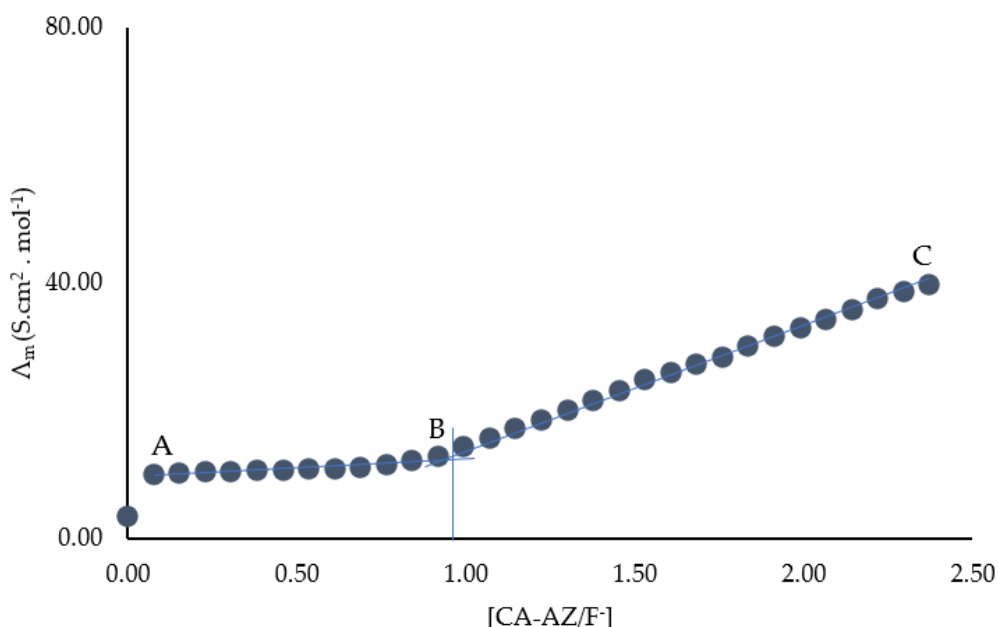
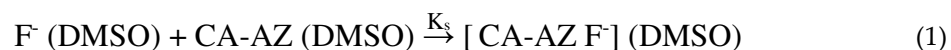


Figure 7. Conductometric titration of CA-AZ with F⁻ in DMSO at 298.15 K.

2.7. Thermodynamics of complexation of CA-AZ with fluoride in DMSO at 298.15 K

The isolation of the fluoride complex salt requires quantitative data on its stability. It should be noted that despite the importance of thermodynamics in assessing quantitatively the selectivity of azo-calix[4]arenes for ionic species in a given medium, hardly any such study have been reported in the literature. Therefore, calorimetric titrations of CA-AZ with F⁻ in DMSO were conducted. Thus, the stability constant ($\log K_s$), hence ($\Delta_c G^\circ$), enthalpy ($\Delta_c H^\circ$) and entropy ($\Delta_c S^\circ$) of the complexation were calculated and these data are reported in Table 3. The data are referred to the process represented in Eq.1.



Where [CA-AZ F⁻] denotes the anion complex. The data indicate that the fluoride complex is rather stable and its stability results from the favorable contribution of both, the enthalpy and the entropy, but the process is entropically controlled. The positive entropy is likely to be attributed to the desolvation of the anion or the receptor or both upon complexation. Attempts were made to determine the thermodynamic parameters of CA-AZ with other anions, but the heats obtained were very small to derive accurate stability constant values. Approximate values obtained clearly indicated that the stability of complexes with chloride and hydrogen sulphate were relatively weak as compared to the fluoride complex. We were unable to establish the thermodynamics associated with the binding process involving hydrogen phosphate given that the composition of the complex could not be accurately established.

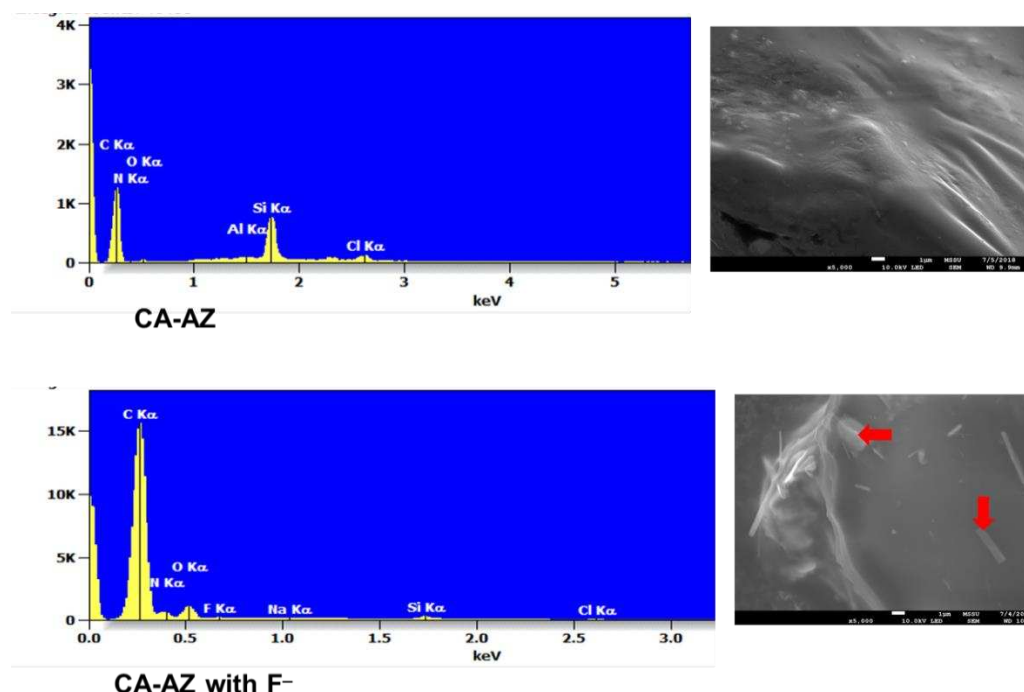
Table 3. Thermodynamic parameters of complexation of *para*-ester diazophenylcalix[4]arene and fluoride in DMSO at 298.15 K.

| <i>para</i> -ester diazophenylcalix[4]arene | | | | | |
|---|--------------------|---------------|--------------------------------------|--------------------------------------|---|
| Anion | (CA-AZ: M^{n-}) | $\log K_s$ | $\Delta_c G^\circ$ (kJ mol $^{-1}$) | $\Delta_c H^\circ$ (kJ mol $^{-1}$) | $\Delta_c S^\circ$ (J mol $^{-1}$ K $^{-1}$) |
| F $^-$ | 1:1 | 5.9 \pm 0.1 | -33.7 \pm 0.2 | -12 \pm 0.3 | 72 |

Having established the stability of the fluoride complex we proceeded with its isolation and characterization of the complex salt as described below.

2.8. SEM-EDX and FT-IR Characterization of Bu $_4$ N [CA-AZ F]

SEM provides the morphological characteristics of the compound whereas EDX generates its elemental composition. Inspection of the micrographs of CA-AZ and CA-AZ loaded with F $^-$ (Figure 8) shows the presence of the ion (red arrows) in the compound. A change in the morphology of its surface is also found which is referred to the complexation of the compound with the fluoride ion. Regarding the EDX spectra, the characteristic peaks of the CA-AZ are shown while for the CA-AZ - F $^-$ salt spectrum, an additional peak for fluoride is present that is attributed to the presence of fluoride in the compound. The increase in the carbon peak is due to the presence of tetrabutylammonium salt.

**Figure 8.** Morphological micrographs of azocalix[4]arene (CA-AZ) and azocalix[4]arene loaded with fluoride ion (red arrows) with corresponding EDX spectra showing the elemental composition. X 5,000 original magnification, Al peak corresponds to aluminum stub used for samples' mounting.

The azocalix[4]arene and the fluoride complex salt also assessed *via* FTIR recorded in the range 4000-500 cm $^{-1}$ are displayed in Figure 9. The characteristic peaks which are attributed to the phenol OH stretching are shown in both spectra (A and B) as broad bands at 3253 cm $^{-1}$ for the compound and 3380 cm $^{-1}$ for fluoride complex salt. The bands at 2996 and 2954 cm $^{-1}$ in A and B spectra are referred to C-H stretching vibration of CH $_2$ in azocalix[4]arene and its fluoride complex salt. Inspecting the characteristic peak positions in both spectra, a blue shift of +127 cm $^{-1}$ in the OH band is observed with a reduced intensity and a red shift of -42 cm $^{-1}$ in C-H band with an increased intensity

indicating an interaction between the compound and a fluoride ion. Also, three bands at 1713, 1471 and 1271 cm^{-1} correspond to C=O, N=N and C-O vibration in azocalix[4]arene are red shifted to 1629, 1459 and 1201 cm^{-1} with decreased intensity upon the interaction of the compound with fluoride salt. Interestingly, the strong band at 1010 cm^{-1} in CA-AZ corresponding to the C-OH vibration almost disappeared from the complex salt spectrum due to a deprotonation of the compound caused by F^- , leading to a blue shift in the OH band of the complex.

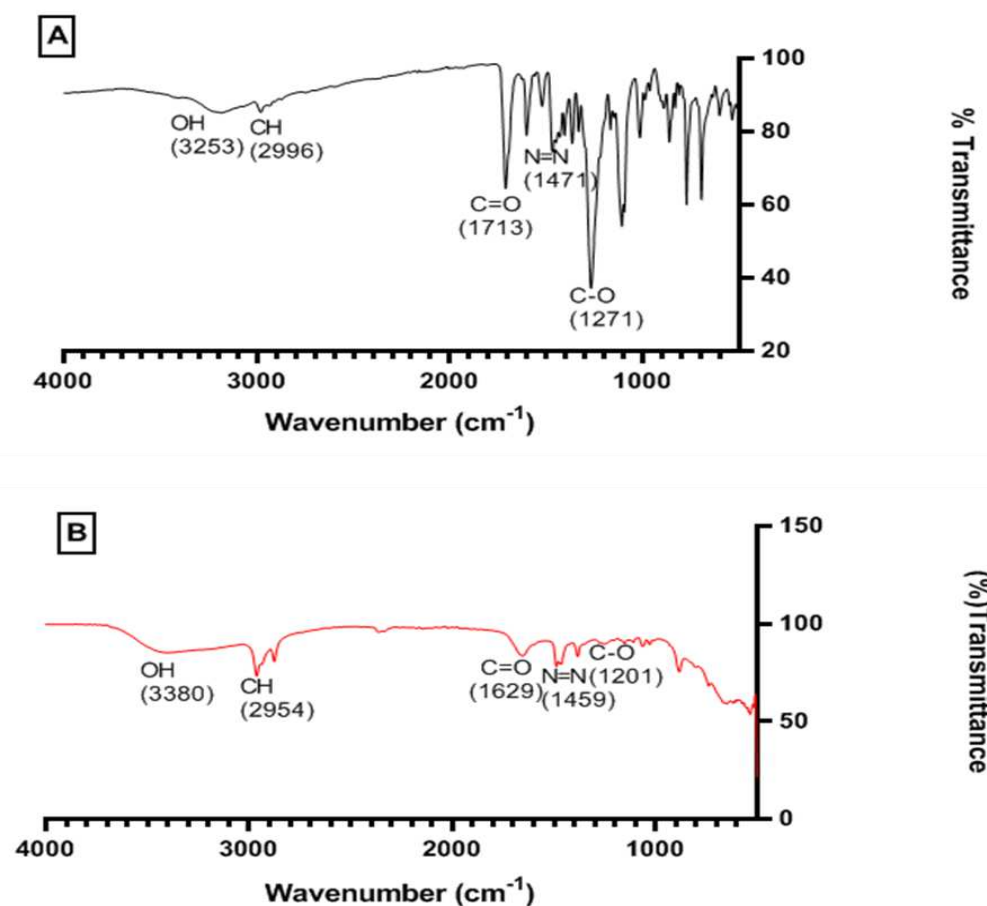


Figure 9. FTIR spectra of A, azocalix[4]arene and B, azocalix[4]arene loaded with TBAF.

2.9. Interaction of $\text{Bu}_4\text{N}[\text{CA-AZ F}]$ with CO_2

The CA-AZ was designed to host and sense ionic species, but upon isolating the $\text{Bu}_4\text{N}[\text{CA-AZ F}]$ salt it was discovered that while the free receptor does not interact with CO_2 , the fluoride salt does. It detects and captures CO_2 from air where the colour changes from red to orange yellow (Figure 10). The process of the gas detection by the complex salt was established within seven seconds. These observations were further investigated by FTIR studies to explore the mode of interaction with CO_2 .

The infrared spectrum of the solid complex salt is shown in Figure 10. The assignment of the bands was referred to data available for relevant compounds [49 & 50]. Characteristic bands of the complex salt were explained in section 2.8. However, the broad band at 3345 cm^{-1} which is assigned to the -OH stretching vibrations of the phenol ring in the solid complex was redshifted with an increased intensity and less broadened upon the complex exposure to CO_2 . Moreover, the band at 1675 cm^{-1} , attributed to the C=O vibration was redshifted to 1650 cm^{-1} as it got sharper upon the interaction of the complex salt with carbon dioxide. Inspecting the C=O band of the complex, it is noticed the broadness of the signal when compared with the one of the CO_2 treated complex. Hellwig [62] explained that the broadening band of the C=O results from its interaction with water. We are strongly of the view that unlike the free receptor, the fluoride complex salt is highly hygroscopic and as such the presence of water promotes the interaction of the fluoride complex salt with CO_2 . No

shifts were observed in the bands at 1457 and 1251 cm^{-1} which correspond to the N=N and the C-O stretching vibrations in the spectrum of the carbon dioxide loaded probe. Moreover, the IR spectrum of the probe with carbon dioxide shows a peak at 2327 cm^{-1} which is attributed to the gas.

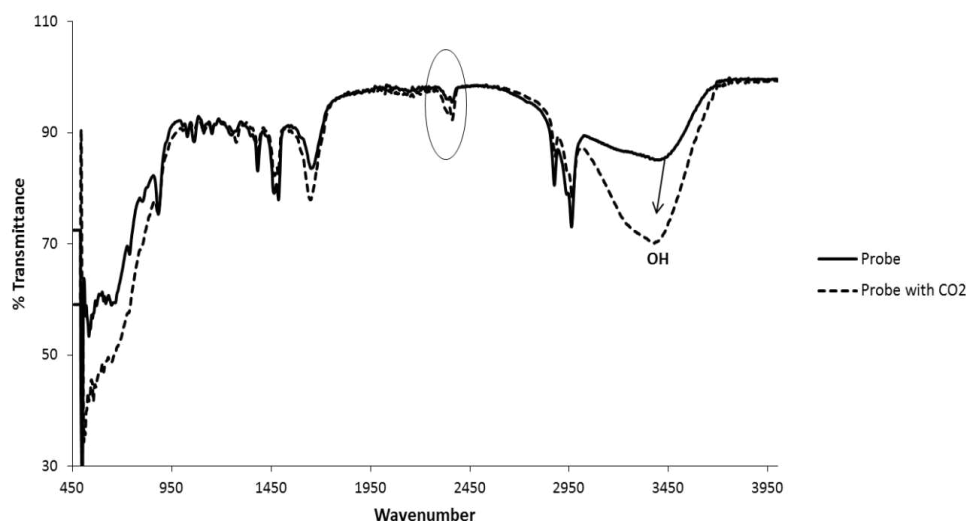


Figure 10. FTIR spectra of the solid probe (blue) (a) probe with carbon dioxide (red) (b) probe saturated with carbon dioxide (yellow)(c).

2.9.1. Extraction of carbon dioxide by the solid complex salt

The solid complex salt ($\text{Bu}_4\text{N} [\text{CA-AZ F}]$) was nourished with CO_2 gas in a fix bed reactor where the extraction percentage was recorded at different time intervals (Figure 11). Inset in Figure 11 shows an increase in the percentage removal of CO_2 from the air which started after 18 seconds where it reached 68 % after 44 seconds.

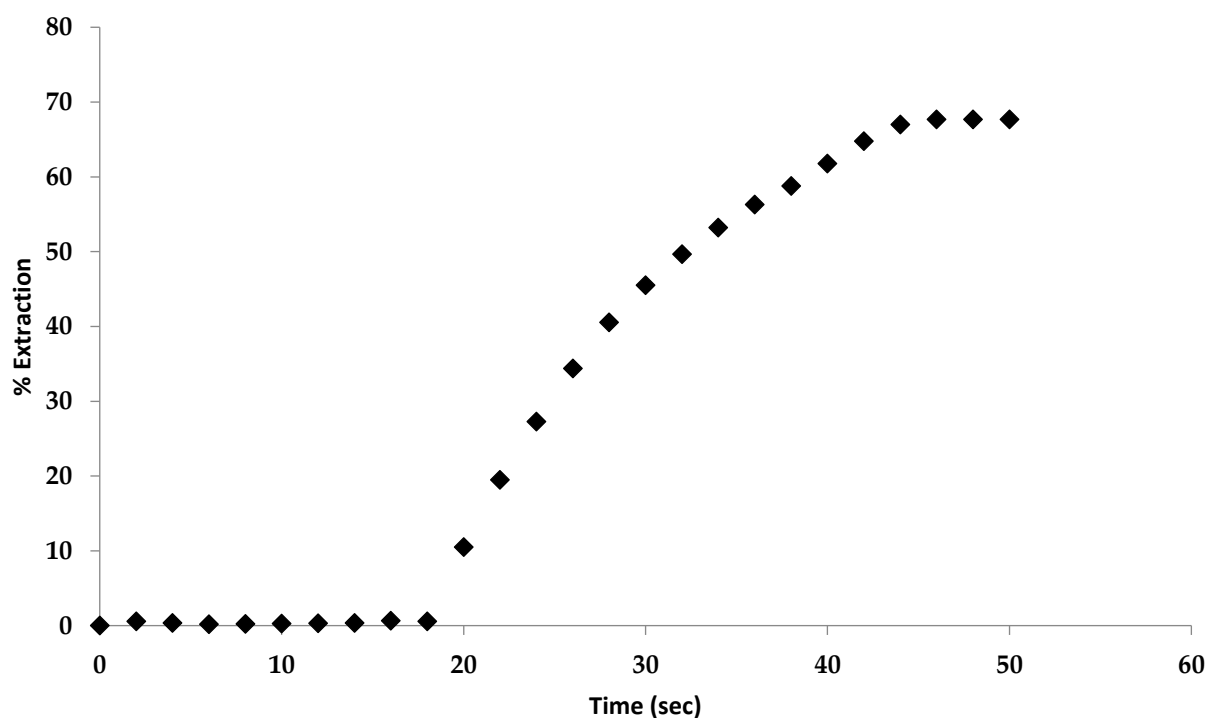


Figure 11. Plot showing of percentage of carbon dioxide extraction by the complex versus time (seconds).

2.9.2. Recycling of the complex

Carbon dioxide was able to be removed from the complex salt when purged with nitrogen gas for three minutes or placed under vacuum where it retained its original colour (dark blue). The dark blue colour of the complex salt means that it has zero carbon dioxide and this will not be observed unless it is placed under vacuum (Figure 12a). However, when the solid complex salt was exposed to carbon dioxide, the color changed to red and then to yellow with more CO₂ exposure where no more colour change was observed after, which indicates the saturation of the solid complex salt with carbon dioxide (Figure 12). Interestingly, the yellow coloured solid complex was recycled back to dark blue when it was placed under vacuum.

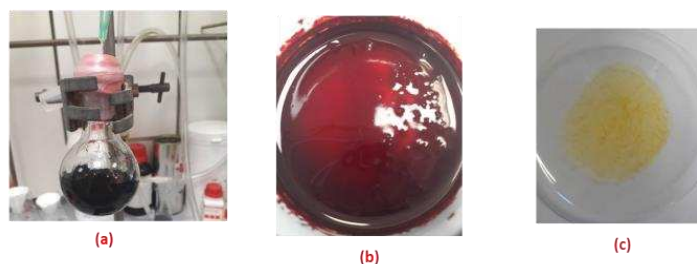


Figure 12. Recycled solid complex salt placed under vacuum (a); complex salt initially exposed to CO₂ (b); complex salt fully exposed to CO₂ (c).

3. Materials and Methods

3.1. Chemicals

All chemicals used throughout the work were of analytical grade. Salts used throughout this study were placed in a vacuum oven and then stored in vacuum desiccators over phosphorus pentoxide, P₄O₁₀ for several days to remove water, before being used for experimental purposes. *p*-*tert*-Butyl calix[4]arene (C₄₄H₅₆O₄, ≥ 97%), ethyl 4-aminobenzoate (H₂NC₆H₄CO₂C₂H₅, 98 %), phenol (C₆H₆O, ≥99 %), sodium ethanoate trihydrate (C₂H₃NaO₂ · 3 H₂O, ≥99%), sodium nitrite (NaNO₂, 97+ %), aluminium (III) chloride (AlCl₃, 98.5%), tetra-*n*-butylammonium chloride ((C₄H₉)₄NCl, ≥97.0%), tetra-*n*-butylammonium fluoride hydrate ((C₄H₉)₄NF · H₂O, 98%), tetra-*n*-butylammonium dihydrogen phosphate ((C₄H₉)₄NH₂PO₄), 97%), tetra-*n*-butylammonium hydrogen sulfate ((C₄H₉)₄NHSO₄, 97%) and potassium carbonate (K₂CO₃, 99+ %) were purchased from Sigma Alrich.

Deuterated solvents used in NMR experiments, dimethyl sulfoxide-*d*₆ (C₂D₆OS, 99.9%), and chloroform-*d* (CDCl₃, 99.8% + 0.05 % v/v TMS) were purchased from Cambridge Isotope Laboratories.

3.2.1. Synthesis of 25, 26, 27, 28-tetrahydroxy calix[4]arene via de-*tert*-butylation (Friedel Craft de-*tert*-butylation reaction)

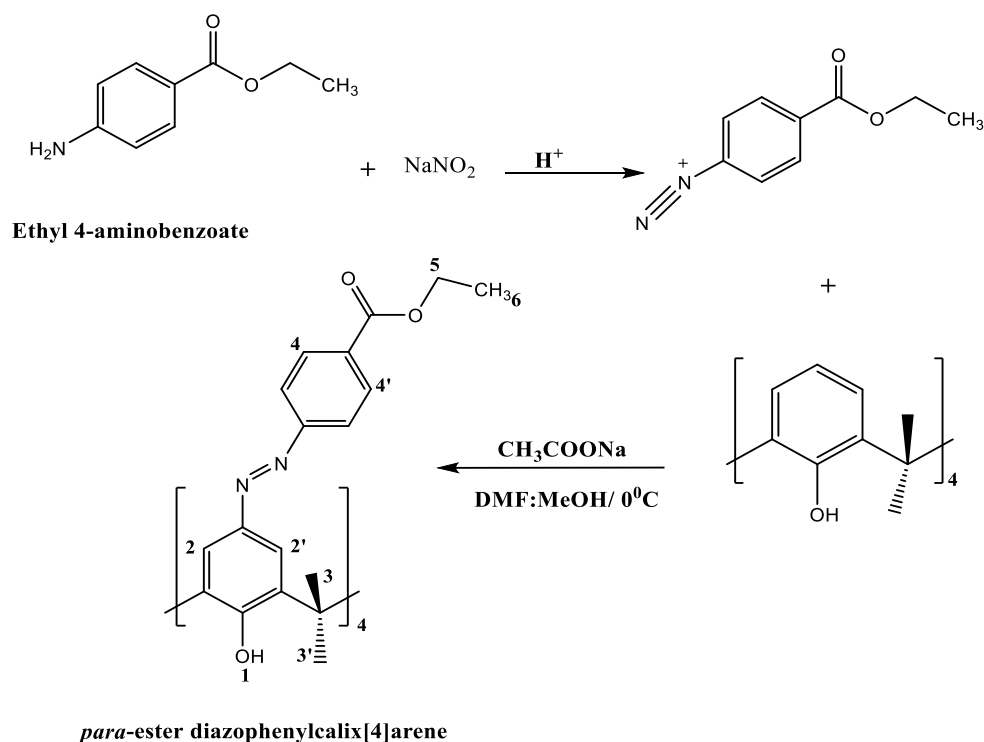
De-*tert*-butylation of the cyclic tetramer was carried out as previously reported [63,64].

The product was characterized by ¹H NMR at 298 K to give the following signals:

¹H NMR (500 MHz, CDCl₃, δ in ppm); 10.19 (s, OH, 4 H (1)); 7.04 (d, Ar-H, 8 H (3)); 6.7 (t, Ar-H, 4 H (2 & 2')); 4.26 (d, H-axial, 4 H (4)); 3.48 (d, H-equatorial, 4 H (4')).

3.2.2. Preparation of 5,11,17,23-tetra[(4-ethylacetoxypheyl) (azo)]calix[4]arene, CA-AZ

The compound was synthesized by a diazotization reaction [65] described in Scheme I.



Scheme 1. Synthetic procedure used for the preparation of CA-AZ.

In a 500 cm³ round-bottomed flask, ethyl 4-aminobenzoate (1.29 g, 7.8 mmol), sodium nitrite (0.41 g, 6.00 mmol) and conc. HCl (14 cm³) in water (25 cm³) was added gradually to a cold solution (0-5 °C) of 25, 26, 27, 28-tertrahydroxy calix[4]arene (0.64 g, 1.5 mmol) and sodium ethanoate trihydrate (1.17 g, 8.6 mmol) in a DMF/MeOH (2:1) mixture to obtain a dark orange colored suspension. The mixture was stirred for 6 hours; a red precipitate was observed. The mixture was filtered, and the residue was washed with cold water then methanol several times. The product was left on the Schlenk line for one week. (0.63 g, 98 % yield).

The product was characterized by ¹H NMR (500 MHz) at 298 K.

¹H NMR (500 MHz, CDCl₃, δ in ppm); 10.25 (s, OH, 4 H (**1**)); 8.13 & 8.14 (d, Ar-H, 8 H (**4** & **4'**)); 7.85 (s, Ar-H, 4 H (**2** & **2'**)); 4.39 (q, COO-CH₂-CH₃, 8 H (**5**)); 4.4 (d, H-axial, 4 H (**3**)); 3.87 (d, H-equatorial, 4 H (**3'**)); 1.4 (t, CH₃, 12 H (**6**)).

Elemental analysis was carried out in duplicate at the University of Surrey; (C₆₄H₅₆N₈O₁₂) MW. (1129.20); Calculated %; C, 68.08; H, 5.0; N, 9.92. Found %; C, 68.14; H, 4.93; N, 10.2.

3.3. FT-IR, Thermogravimetric and SEM-EDX analyses of CA-AZ and CA-AZ-F⁻ salt

Compound (CA-AZ) and fluoride loaded CA-AZ were analysed *via* Fourier Transform Infrared Spectroscopy (using an Agilent Cary 600 Series FT-IR spectrometer). Measurements were made within the 4000 to 600 cm⁻¹ range. Calibration spectra were made from 32 scans. The FT-IR spectra were scanned against air background spectrum. For CA-AZ thermal stability, analysis were recorded using a thermogravimetric analyser (TGA Q500 V6.7) under nitrogen gas. Sample was heated from 25 °C to 800 °C at a heating rate of 10 °C/min.

Regarding SEM-EDX measurements, a scanning electron microscope (SEM) JEOL JSM-7100F, equipped with secondary and backscattered imaging coupled with Ultradry energy dispersive X-ray (EDX) for elemental analysis was used for morphological investigations. CA-AZ treated with fluoride ion samples were mounted on an aluminium stub. Working conditions were 15 KeV for accelerating voltage and 10 mm for the detector working distance.

3.4. ^1H NMR complexation studies

^1H NMR complexation experiments were conducted at 298 K by dissolving the ligand (2.17×10^{-4} mol.dm $^{-3}$) in DMSO- d_6 , then adding a known amount of the salt (1.10×10^{-3} mol.dm $^{-3}$) into an NMR tube using TMS as an internal standard. Chemical shift changes ($\Delta\delta$, ppm) were calculated by subtracting the chemical shift of the free ligand (reference spectrum) from the chemical shift of the complex. Chemical shift changes ($\Delta\delta$) values greater than 0.1 ppm are an indication of an interaction that requires further investigations.

3.5. UV-Visible studies of CA-AZ and ion salts in dimethyl sulfoxide

UV-Visible studies were carried out by Thermo Scientific Evolution 220 UV-Visible Spectrophotometer. Data was processed with INSIGHT software. Quartz cuvette cell was used for sample measurement. Absorbances were recorded over a wavelength range of 350- 750 nm.

The selectivity of the synthesized calix[4]arene derivative along with its chromogenic properties were investigated using stock solutions of the ligand (1×10^{-5} mol dm $^{-3}$) and the anion salt (CO_3^{2-} , F^- , H_2PO_4^- , HSO_4^- & Cl^-) (1×10^{-4} mol dm $^{-3}$), (ammonium and potassium as counter-ions for carbonate and tetra-n-butyl ammonium as counter-ion for other anions) in dimethyl sulfoxide. Screening experiments on different cation and anion salt solutions were carried out prior to this step. A CA-AZ solution (3 cm 3) was placed in quartz cell and the absorbance spectrum was recorded against DMSO. UV-absorption measurements of the complex (ligand- ion salt) were also conducted in a solution (3 cm 3) containing the same concentration of the ligand with the desired amount of salt solutions.

3.6. ^1H NMR titration studies

^1H NMR titration of *para*-ester diazophenylcalix[4]arene with F^- was carried out. The reference sample (0.5 cm 3 , 1×10^{-4} mol dm $^{-3}$) was prepared in deuterated dimethyl sulfoxide and another solution of the anion salt was made at a concentration of 2×10^{-4} mol dm $^{-3}$ in 2 cm 3 of the same solvent. ^1H NMR measurements were performed for the reference sample, then aliquots of the anion salt were added stepwise (9 additions for each anion of 40 μl) and measurements were carried out following each addition. Chemical shift changes ($\Delta\delta$) were calculated.

3.7. Conductometric titrations of *para*-ester diazophenylcalix[4]arene and fluoride anion in dimethyl sulfoxide at 298.15 K

For conductometric titration experiments, a solution of fluoride ion salt in dimethyl sulfoxide (25 cm 3) was prepared and transferred to the conductometric cell. Then, the electrodes were inserted, and the solution was stirred for a few minutes until thermal equilibrium was established. Afterwards, the ligand solution prepared in the same solvent was added stepwise until stable readings were observed. The reciprocal of resistance, L (Ω^{-1}) was calculated following each addition. The molar conductance was then calculated as previously [66].

3.8. Calorimetric titration experiments

Calorimetric titration experiments (direct) were carried out in dry dimethyl sulfoxide at 298.15 K as previously described [67].

3.9. Carbon dioxide detection studies by *para*-ester diazophenylcalix[4]arene-fluoride complex using FTIR.

FTIR was the analytical technique used in this section to determine the sensitivity and complexation of the carbon dioxide gas with solid *para*-ester diazophenylcalix[4]arene-fluoride complex.

The solid complex salt was prepared in a film in THF solvent then the solvent was evaporated, and the complex salt was exposed to carbon dioxide where FT-ATR measurements were made. The spectrum was recorded as described in section 3.3.

3.9.1. Extraction of CO₂ by the solid complex salt

A sample of the solid complex salt (1.2 g) was deposited on a quartz wool where it was placed in a tubular fixed-bed quartz reactor. The experiment was performed at atmospheric pressure, and the temperature was controlled by a thermocouple. The outlet gas (CO₂) was monitored by infrared and thermal conductivity detectors on an ABB AO2020 online gas analyzer. The outlet total volumetric rate of the gas was measured by a flow meter.

4. Conclusions

The results presented in this paper illustrates important features about the properties of the azocalix[4]arene derivative such as

- i) The conformational change that the receptor undergoes as a result of the medium effect and complexation with anions in DMSO.
- ii) The fast kinetics of anion complexation reflected in the immediate colour change resulting from the receptor-anion interaction easily detected by a naked eye
- iii) The selectivity of the receptor for fluoride is demonstrated to an extent that unlike for other anions, the stability of the fluoride complex was quantitatively assessed through titration calorimetry. Furthermore, the process is entropy controlled because of the de-solvation of the anion or receptor or both, upon complexation.
- iv) The mode of interaction of the receptor with the anion was established and consisted of deprotonation of one of the phenolic units in the narrow rim of the receptor followed by protonation of the functionalised upper rim which provide the sites of interaction with the anion
- v) The ability of the fully characterized anion salt to remove CO₂ from the air is illustrated through the text, together with the recycling of the complex salt. This is a very important aspect to highlight given that so far, most reports on calixarene chemistry are centered on the complexation process but there is a need to explore further the practical applications of macrocyclic complex salts.

Author Contributions: “Conceptualization, A.F. Danil de Namor; methodology, N. Al Hakawati; software, N. Al Hakawati; validation, A.F. Danil de Namor and N. Al Hakawati; formal analysis, A.F. Danil de Namor; investigation, A.F. Danil de Namor and N. Al Hakawati; writing—original draft preparation, N. Al Hakawati; writing—review and editing, A. F. Danil de Namor; supervision, A.F. Danil de Namor; All authors have read and agreed to the published version of the manuscript.”

Funding: “N. A. is thankful to be late Dr. Melhem Namor for his financial support provided to the project and the authors would like to dedicate this paper to his memory”.

Acknowledgments: The authors thank Prof. John Watts and his staff for invaluable assistance in the use of the SEM equipment available in the Micro Structural Unit and Surface Analysis Laboratory (University of Surrey).

Conflicts of Interest: “The authors declare no conflict of interest.”

References

1. Schrag, P.D. Preparing to capture Carbon. *Science* **2007**, *315*, 812-13.
2. Li, L.; Zhao, N.; Wei, W.; Sun, Y. A Review of research progress on CO₂ capture, storage and utilization I Chinese Academy of Sciences. *Fuel* **2013**, *108*, 112-130.
3. Dawson, R.; Cooper, A.I.; Adams, D.J. Chemistry functionalization strategies for carbon dioxide capture in microporous organic polymers. *Polymer Int.* **2013**, *62*, 335-522.
4. Perry S.F.; Abdallah, S. Mechanisms and consequences of carbon dioxide sensing in fish. *Respir. Phys. Neurobiol.* **2012**, *184*, 309-315.
5. Neethirajan, S.; Jayas, D.S.; Sadistap, Carbon dioxide (CO₂) sensors for the Agri-Food Industry- A Review. *Food Bioprocess Technol.* **2009**, *2*, 115-21.
6. Puligundla, P.; Jung, J.; Ko, S. Carbon dioxide sensors for Intelligent food packaging. *Food Control* **2012**, *25*, 328-333.
7. Mills, A.; Lepre, A.; Wild, L. Breath-by-Breath Measurements of carbon dioxide using a plastic film optical sensor, *Sens. Actuators, B* **1997**, *38*, 419-.

8. Yasuda, T.; Yonemura, S.; Tani, A. Comparison of the characteristics of small commercial NDIR CO₂ of a portable CO₂ measurement device. *Sensors* **2012**, *12*, 3641-55.
9. Vorotyntsev, V.M.; Mochalov, G.M.; Baranova, I.V.; Gas Chromatographic determination of admixtures of permanent gases CO, CO₂ and hydrocarbons in methyl silane. *J. Anal. Chem.* **2013**, *68*, 152-55.
10. Xie, X.; Bakker, E. Non-Severinghaus Potentiometric Dissolved CO₂ sensor with improved characteristics. *Anal. Chem.* **2013**, *85*, 1332-36.
11. Beyenal, H.; Davis, C.C.; Lewandowski, Z. An improved Severinghaus type carbon dioxide microelectrode for use in biofilms. *Sens. Actuators, B* **2004**, *97*, 202-210.
12. Lee, M.; Jo, S.; Lee, D.; Xu, Z.; Yoon, J. A new naphthalimide derivative as a selective fluorescent and colorimetric sensor for fluoride, cyanide and CO₂. *J. Dyes and Pigments* **2015**, *120*, 288-292.
13. Gupta, R.C.; Ali, R.; Razi, S.S.; Srivastava, P.; Dwivedi, S.K.; Misra, A. Synthesis and Applications of a new class of D- π -A type charge transfer probe containing imidazole-naphthalene units for detection of F⁻ and CO₂. *RSC Adv.* **2017**, *7*, 4941-49.
14. Xia, G.; Ruan, C.; Wang, H. Highly sensitive detection of carbon dioxide by a pyramido (1,2-a) benzimidazole derivative combining experimental and theoretical studies. *Analyst* **2015**, *140*, 5099-5104.
15. Xia, G.; Liu, Y.; Ye, B.; Sun, J.; Wang, H. A squaraine-based colorimetric and F⁻ dependent chemo sensor for recyclable CO₂ gas detection: highly sensitive off-on-off response. *J. Chem. Soc. Chem. Commun.* **2015**, *51*, 13802-805.
16. Gutsche, C.D. Calixarenes. The Royal Society of Chemistry **1969**.
17. Danil de Namor, A.F.; Cleverley, R.M.; Zapata Ormachea, M.L. Thermodynamics of Calixarene Chemistry. *Chem. Reviews* **1998**, *98*, 2495-2525.
18. Danil de Namor, A.F.; Chahine, S.; Castellano, E.E.; Piro, O.E.; Jenkins, H.D.B. A Preliminary Observation of Additive Thermodynamic Contribution of Pendant Arms to the Complexation of Calixarene Derivatives with Mercury (II). *J. Chem. Soc. Chem. Comm* **2005**, 3844-3846.
19. Danil de Namor, A.F.; Chahine, S. The Effect of Solvation of Guest, Supramolecular Host and Host-Guest Complex on the Thermodynamic Selectivity of Calix [4] arene Derivatives and Soft Metal Cations. *J. Phys. Chem* **2005**, *109*, 18096-112.
20. Danil de Namor, A.F.; El Gamouz, A.; Alharthi, S.; Al Hakawati, N.; Varcoe, J.R. A Ditopic Calix [4] pyrrole Amide Derivative: Highlighting the Importance of Fundamental Studies and the Use of NaPh4B as Additive in the Design and Applications of Mercury (II) Ion Selective Electrodes. *J. Mater. Chem. A* **2015**, *3*, 13016-13030.
21. Danil de Namor, A.F.; Alharthi, S.; El Gamouz, A.; Al Hakawati, N.; Cox, B.G. Calix [4] Based Hg (II) Ion Selective Electrodes: A Thermodynamic Protocol to Address the Selectivity versus the hosting capacity paradigm in the selection of the carrier. *Electrochimica Acta* **2018**, *290*, 686-694.
22. Benkhaya, S.; Mrabet, S.; El Harfi, A. Classifications, properties, recent synthesis and applications of azo dyes. *Heliyon* **2020**, *6*, e03271. doi: 10.1016/j.heliyon.2020.e03271.
23. Benkhaya, S.; Cherkaoui, O.; Assouag, M.; Mrabet, S.; Rafik, M.; El Harfi, A. Synthesis of a New Asymmetric Composite Membrane with Bi-Component Collodion: Application in the Ultra filtration of Baths of Reagent Dyes of Fabric Rinsing/Padding. *J. Mater. Environ. Sci.* **2016**, *7*, 4556-4569.
24. Georgiev, A.; Stoilova, A.; Dimov, D.; Yordanov, D.; Zhivkov, I.; Weiter, M. Synthesis and photochromic properties of some N-phthalimide azo-azomethine dyes. A DFT quantum mechanical calculation on imine-enamine tautomerism and trans-cis photoisomerization. *Spectrochim. Acta A Mol. Biomol. Spectrosc.* **2019**, *210*, 230-244.
25. Sahan, F.; Kose, M.; Hepokur, C.; Karakas, D.; Kurtoglu, M. New azo-azomethine-based transition metal complexes: Synthesis, spectroscopy, solid-state structure, density functional theory calculations and anticancer studies. *Appl. Organomet. Chem.* **2019**, *33*, e4954.
26. Oueslati, F.; Dumazet-Bonnamour, I.; Lamartine, R. New Azothiacalix[4]arenes Containing Biheterocyclic Subunits: Extraction and Complexation Properties. *Supramol. Chem.* **2004**, 227-232.
27. Gunnlaugsson, T.; Leonard, J.P.; Murray, N.S. Highly selective colorimetric naked-eye Cu (II) detection using an azobenzene chemosensor. *Org. Lett.* **2004**, *6*, 1557-1560.
28. Lee, S.J.; Jung, J.H.; Seo, J.; Yoon, I.; Park, K.M.; Lindoy, L.F.; Lee, S.S. A Chromogenic Macrocyclic Exhibiting Cation-Selective and Anion-Controlled Colour Change: An Approach to Understanding Structure-Color Relationships. *Organic. Letts.* **2006**, *8*, 1641-1643.
29. Cheng, Y.F.; Zhao, D.T.; Zhang, M.; Liu, Z.Q.; Zhou, Y.F.; Shu, T.M.; Li, F.Y.; Yi, T.; Huang, C.H. Azo 8-hydroxyquinoline benzoate as selective chromogenic chemo sensor for Hg²⁺ and Cu²⁺. *Tetrahedron Lett.*, **2006**, *47*, 6413-6416.
30. Lee, S.J.; Lee, S.S.; Jeong, I.Y.; Lee, J.Y.; Jung, J.H. Azobenzene coupled chromogenic receptors for the selective detection of copper (II) and its application as a chemo sensor kit²⁴. *Tetrahedron Lett.* **2007**, *48*, 393-396.
31. Lee, J.H.; Lee, H.Y.; Lee, D.H.; Hong, J.I. Fluoride-selective chromogenic sensors based on azophenol. *Tetrahedron Lett.* **2001**, *42*, 5447-49.

32. Lee, D.H.; Lee, K.H.; Hong, J.I. An Azophenol-based Chromogenic Anion Sensor. *Org. Lett.* **2001**, *3*, 5-8.
33. Lee, D.H.; Lee, H.Y.; Lee, K.H.; Hong, J.I. Selective anion sensing based on a dual-chromophore approach. *Chem. Commun.* **2001**, 1188-89.
34. Lee, D.H.; Im, J.H.; Son, S.U.; Chung, Y.K.; Hong, J.I. An azophenol-based chromogenic pyrophosphate sensor in water. *J. Am. Chem. Soc.* **2003**, *125*, 7752-7753.
35. Sancenón, F.; Martínez-Máñez, R.; Soto, J. A Selective Chromogenic Reagent for Nitrate. *Angew. Chem. Int. Ed.* **2002**, *41*, 1416-1417.
36. Cho, E.J.; Ryu, B.J.; Lee, Y.J.; Nam, K.C. Visible Colorimetric Fluoride Ion Sensors. *Org. Lett.* **2005**, *7*, 2607-2609.
37. Farinha, A.S.F.; Tome, A.C.; Cavaleiro, J.A.S. Synthesis of new calix[4]pyrrole derivatives via 1,3-dipolar cycloadditions. *Tetrahedron* **2010**, *66*, 7595-7599.
38. Yoo, J.; Kim, M.S.; Hong, S.J.; Sessler, J.L.; Lee, C.H. Selective Sensing of Anions with Calix[4]pyrroles Strapped with Chromogenic Dipyrrolylquinoxalines. *J. Org. Chem.* **2009**, *74*, 1065-1069.
39. Suksai, C.; Tuntulani, T. Chromogenic anion sensors. *Chem. Soc. Rev.* **2003**, *32*, 192-202.
40. Chang, K.C.; Su, I.H.; Wang, Y.Y.; Chung, W.S. A Bifunctional Chromogenic Calix[4]arene Chemo sensor for Both Cations and Anions: A Potential Ca^{2+} and F⁻ Switched Inhibit Logic Gate with a YES Logic Function. *Eur. J. Org. Chem.* **2010**, 4700-4704.
41. Quinlan, E.; Matthews, S.E.; Gunnlaugsson, T.J. Colorimetric Recognition of Anions Using Preorganized Tetra-Amidourea Derived Calix[4]arene Sensors. *Org. Chem.* **2007**, *72*, 7497-7503.
42. Kim, H.J.; Kim, S.K.; Lee, J.Y.; Kim, J.S. Fluoride-Sensing Calix-luminophores Based on Regioselective Binding. *J. Org. Chem.* **2006**, *71*, 6611-6614.
43. Wagner-Wysiecka, E.; Lukasik, N.; Biernat, J.F.; Luboch, E. Azo group(s) in selected macrocyclic compounds. *J. Incl. Phenom. and Macrocycl. Chem.* **2018**, *90*, 189-257.
44. Browne, D.; Whelton, H.; Mullane, D.O. Fluoride metabolism and fluorosis. *J. Dent.*, **2005**, *33*, 177-86.
45. Schwarzenbach, B.I.; Escher, K.; Fenner, T.B.; Hofstetter, C.A.; Johnson, U.; von Gunten, B.; Wehrli, The challenge of micropollutants in aquatic systems. *Science* **2006**, *313*, 1072-77.
46. Bassin, E.B.; Wypij, D.; Davis, R.B. Age-specific fluoride exposure in drinking water and osteosarcoma (United States). *Canc. Causes Contr.* **2006**, *17*, 421-28.
47. Danil de Namor, A.F. The Fluoride Dilemma: Thermodynamics of Anion Complexation by Calixpyrroles. *J. Therm. Anal* **2007**, *87*, 7-14.
48. Bazzicalupi, C.; Bencini, A.; Bencini, A.; Bianchi, A.; Corana, F.; Fusi, V.; Giorgi, C.; Paoli, P.; Paoletti, P.; Valtancoli, B.; Zanchini, C. CO₂ fixation by novel copper (II) and zinc (II) macrocyclic complexes. A solution and solid state study. *Inorg. Chem.* **1996**, *35*, 5540-5548.
49. Gaber, M.; El-Sayed, Y.S.; El-Baradie K.; Fahmy, R.M. Cu (II) complexes of monobasic bi-or tridentate (NO, NNO) azo dye ligands: Synthesis, characterization, and interaction with Cu-nanoparticles. *J. Mol. Struct.* **2013**, *1032*, 185-194.
50. Dincalp, H.; Toker, F.; Durucasu, I.; Avcibasi, N.; Icli, S. New thiophene-based azo ligands containing azo methine group in the main chain for the determination of copper(II) ions. *Dyes and Pigments* **2007**, *75*, 11-24.
51. Chawla, H.M.; Hundal, G.; Singh, S.P.; Upreti, S. Conformational morphosis in azocalix[4]arenes. *CrystEngComm*, **2007**, *9*, 119-122.
52. Ho, I.T.; Lee, G.H.; Chung, W.S. Synthesis of Upper-Rim Allyl- and p-Methoxyphenylazocalix[4]arenes and Their Efficiencies in Chromogenic Sensing of Hg²⁺ Ion. *J. Org. Chem.* **2007**, *72*, 2434-2442.
53. Kim, J.S.; Shon, O.J.; Lee, J.K.; Lee, S.H.; Kim, J.Y.; Park, K.M.; Lee, S.S. Chromogenic Azo-Coupled Calix[4]arenes. *J. Org. Chem.* **2002**, *67*, 1372-1375.
54. Kim, J.K.; Kim, G.; Kim, C.R.; Lee, S.H.; Lee, J.H.; Kim, J.S. UV Band Splitting of Chromogenic Azo-Coupled Calix[4]crown upon Cation Complexation. *J. Org. Chem.* **2003**, *68*, 1933-1937.
55. Karci, F.; Sener, I.; Deligoz, H. Azocalixarenes. 1: synthesis, characterization and investigation of the absorption spectra of substituted azocalix[4]arenes. *Dyes Pigments* **2003**, *59*, 53-61.
56. Kim, T.H.; Kim, S.H.; Tan, L.V.; Seo, Y.J.; Park, S.Y.; Kim, H.; Kim, J.S. Transition Metal Ion Selective Ortho-Ester Diazophenylcalix[4]arene. *Talanta* **2007**, *71*, 1294-1297.
57. Chawla, H.; Gupta, T. Design, synthesis and evaluation of a new calix[4]arene based molecular receptor for multiple ion selectivity. *J. Incl Phenom Macrocycl Chem.* **2015**, *81*, 49-56.
58. Löhr, H.G.; Vögtle, F. *Acc. Chem. Rev.* **1985**, *18*, 65.
59. Chen, C.F.; Chen, Q.Y. Azocalix[4]arene-based chromogenic anion probes. *New J. Chem.* **2006**, *30*, 143-147.
60. Thiampanya, P.; Muangsins, N.; Pulpoka, B. Azocalix[4]arene Strapped Calix[4]pyrrole: A Confirmable Fluoride Sensor. *Org. Lett.* **2012**, *14*, 4050-4053.
61. Zheng, Y. L.; Hong, K. S.; Hong, X.; Tong, Y. Y.; Tangxin, X.; Xiao, Q. S.; Juli, J.; Leyong, W. Calix[4]arene containing thiourea and coumarin functionality as highly selective fluorescent and colorimetric chemosensor for fluoride ion. *Spectrochimic Acta Part A: Molecular and Biomolecular Spectroscopy* **2018**, *200*, 307-312.

62. Hellwig, P. Infrared spectroscopic markers of quinones in proteins from the respiratory chain. *Biochemica et Biophysica Acta* **2015**, *1847*, 126-133.
63. Bocchi, V.; Foina, D.; Pochini, A.; Húngaro, R.; Andreetti, G.D. Synthesis, ^1H NMR, ^{13}C NMR spectra and conformational preference of open chain ligands on lipophilic macrocycles. *Tetrahedron* **1982**, *38*, 373-378.
64. Ungaro, R.; Arduini, A.; Pochini, A.; Reverberi, S. p-t-Butyl-calix[4]arene tetracarboxylic acid. A water soluble calixarene in a cone structure. *J. Chem.Soc. Chem.Comm.* **1984**, 981-982.
65. Shinkai, S.; Araki, K.; Shibata, J.; Tsugawa, D.; Manabe, Autoaccelerative diazo coupling with calix[4]arene: substituent effects on the unusual co-operativity of the OH groups. *O. J. Chem. Soc. Perkin Trans.* **1990**, *1*, 3333-3337.
66. Danil de Namor, A.F.; El Gamouz, A.; Alharthi, S.; Al Hakawati, N.; Varcoe, J. R. A ditopic calix[4]pyrrole amide derivative: highlighting the importance of fundamental studies and the use of NaPh4B as additive in the design and applications of mercury(II) ion selective electrodes. *J. Mater. Chem. A* **2015**, *3*, 13016-13030.
67. Chaaban, J. K.; Al Hakawati, N.; Howlin, B.; Bance-Soualhi, R.; Danil de Namor, A.F. An asymmetric N-rim partially substituted calix[4]pyrrole: Its affinity for Ag(I) and its destruction by Hg(II). *Arab. J. Chem.* **2020**, *13*, 4824-4834.

Disclaimer/Publisher's Note: The statements, opinions and data contained in all publications are solely those of the individual author(s) and contributor(s) and not of MDPI and/or the editor(s). MDPI and/or the editor(s) disclaim responsibility for any injury to people or property resulting from any ideas, methods, instructions or products referred to in the content.